UNIVERSITY of
BRADFORD

Library

The University of Bradford Institutional Repository

http://bradscholars.brad.ac.uk

Link to publisher version: *https://doi.org/10.1039/C4PY01782J*

Citation: Wright DB, Patterson JP, Pitto-Barry, A et al (2015) Tuning the aggregation behavior of pH-responsive micelles by copolymerization. Polymer Chemistry. 6(14): 2761-2768.

PAPER

CrossMark
← click for updates

Tuning the aggregation behavior of pH-responsive micelles by copolymerization†

Daniel B. Wright,[a] Joseph P. Patterson,[a] Anaïs Pitto-Barry,[a] Pepa Cotanda,[a] Christophe Chassenieux,*[b] Olivier Colombani*[b] and Rachel K. O'Reilly*[a]

Amphiphilic diblock copolymers, poly(2-(diethylamino)ethyl methacrylate-*co*-2-(dimethylamino)ethyl methacrylate)-*b*-poly(2-(dimethylamino)ethyl methacrylate), P(DEAEMA-*co*-DMAEMA)-*b*-PDMAEMA with various amounts of DEAEMA have been synthesized by RAFT polymerization. Their micellization in water has been investigated by scattering measurements over a wide pH range. It appeared that the polymers self-assembled into pH sensitive star like micelles. For a given composition, when the pH is varied the extent of aggregation can be tuned reversibly by orders of magnitude. By varying the copolymer composition in the hydrophobic block, the onset and extent of aggregation were shifted with respect to pH. This class of diblock copolymer offers the possibility to select the range of stimuli-responsiveness that is useful for a given application, which can rarely be achieved with conventional diblock copolymers consisting of homopolymeric blocks.

Introduction

In a selective solvent, above a critical aggregation concentration (CAC), amphiphilic block copolymers aggregate by the association of the solvophobic blocks into micellar cores surrounded by a corona made of the solvated solvophilic blocks.[1,2] Vast reports and reviews demonstrate both theoretically and experimentally that the physical and chemical nature of the solvophobic and solvophilic blocks influence the aggregation behavior of the block copolymers.[3–5] However, the extensive library of block copolymer micelles has focused on homopolymeric blocks, these homopolymeric blocks severely restrict self-assembly behavior as it is intrinsically limited to the associative block. Although these homopolymeric diblocks are used successfully for a range of applications, for each new application a new polymer has to be synthesized.

A method to overcome this is to use a copolymer for the associative block; as such, the associative block properties can be tailored dependent on the copolymer composition. It is well established in the literature that to tune the behavior of

stimuli responsive polymers an option is to copolymerize stimuli responsive units with non-responsive or differently responsive ones. For example, it was exhibited that statistical copolymers of pH sensitive and inert monomers exhibited ionization behavior dependent on the non-responsive monomer content.[6] Lutz *et al.* showed that lower critical solubility temperature (LCST) values could be selectively targeted by controlling the statistical copolymer composition.[7,8] However, only a few reports exist where a stimuli responsive copolymer block forms the solvophobic block(s) of the polymer.[9–16] These novel copolymer diblocks resulted in block copolymers whose aggregation and dynamics of self-assembly could be controlled by pH allowing equilibrated structures to form.

Note that many amphiphilic homopolymeric block copolymers form out-of-equilibrium "frozen" structures, a consequence of either a glass transition temperature (T_g) above experimental conditions, restricting core block mobility, or large solvophobicity of the core forming block, producing a large activation energy barrier for molecular exchange regardless of T_g. As such the behavior of these "frozen" micelles also depends to some extent on the way the polymer was dispersed and show little or an irreversible response to external stimuli.[17–19] Furthermore, by copolymerizing responsive units into the associative block the effective solvophobicity is reduced and these novel copolymer diblock polymers can overcome kinetic obstacles and are thermodynamically controlled. This offers improved behavior over conventional frozen homopolymeric blocks as no preparation pathway dependence exists allowing the formation of reproducible equilibrium structures.

[a] University of Warwick, Department of Chemistry, Gibbet Hill Road, Coventry CV4 7AL, UK. E-mail: R.K.O-Reilly@warwick.ac.uk
[b] LUNAM Université, Université du Maine, IMMM UMR CNRS 6283, Département PCI, Avenue Olivier Messiaen, 72085 Le Mans Cedex 09, France.
E-mail: olivier.colombani@univ-lemans.fr, christophe.chassenieux@univ-lemans.fr

These copolymer associative blocks have vast improvements over conventional homopolymeric blocks as a range of responsive behavior can be achieved with subtle changes to the composition. Moreover, the ability to select the responsive behavior opens up the scope of applications for a single block copolymer system in comparison to synthesizing new block copolymers for each application as known for homopolymeric block copolymers.

PDEAEMA, poly(diethylaminoethyl)methacrylate diblock copolymers are used widely in the literature as pH-responsive diblock copolymers in aqueous media, as a consequence of the increase in hydrophobicity upon deprotonation.[20–22] Gast and co-workers have studied poly(dimethylaminoethyl)methacrylate-*block*-poly(diethylaminoethyl)methacrylate, PDMAEMA-*b*-PDEAEMA, polymers in depth and shown that these polymers form spherical micelles in aqueous solution depending on the degree of ionization of the polymer.[23,24] On the other hand, P(DMAEMA) diblock copolymers also show a pH response, but in this case these polymers are permanently hydrophilic and only show a decrease in hydrophilicity upon deprotonation.[6,11,25,26] Therefore, introducing solvophilic units into the solvophobic block, a P(DEAEMA-*co*-DMAEMA)-*b*-PDMAEMA diblock copolymer with a moderately responsive PDEAEMA containing block was targeted. Accordingly, the pH region where the micelles exist can be shifted with respect to the relative copolymer composition of the associative block. Furthermore, the extent of aggregation can be tuned over larger orders of magnitude by slight variations in stimulus, owing to the ultra pH sensitivity of the assemblies. The objective of this work was to both tune the pH region and extent of aggregation for responsive copolymer diblocks into highly sensitive pH responsive micelles using a copolymerization approach. We propose that such a versatile approach increases the scope of the application and understanding of the solution behavior of responsive polymeric micelles.

Experimental

Materials

Monomers were filtered through a plug of silica prior to use and stored at 4 °C. AIBN (2,2′-azo-bis(isobutyronitrile)) was recrystallized from methanol and stored in the dark at 4 °C. All other materials were used as received from Aldrich, Fluka, and Acros. HCl (1 M) and NaOH (1 M) were calibrated and standardized using tris(hydroxymethyl)-aminomethane and potassium hydrogen phthalate respectively.

General procedure for copolymerization of DMAEMA with DEAEMA

A solution of 40 equivalents of a combination of the two monomers (DMAEMA = x, DEAEMA = 40-x), 0.2 equivalents of AIBN and 1 equivalent of 2-cyano-2-propyl dithiobenzoate (CPDB) in 1,4-dioxane (1 : 1 volume compared to monomer) was added to a dry ampoule containing a stirrer bar. The solution was degassed using at least 3 freeze–pump–thaw cycles,

Table 1 Characteristics of the diblock copolymers

Diblock copolymer	x^a	n^b	m^b	$M_{n,NMR}^b$ (kDa)	$M_{n,SEC}^c$ (kDa)	$Đ_{,SEC}^c$	dn/dC^d (mL g^{-1})
1	0.32	35	30	10.7	13.8	1.16	0.125
2	0.65	36	35	12.3	14.2	1.12	0.122
3	0.76	25	34	10.0	12.8	1.18	0.127
4	0.91	28	32	10.4	13.5	1.10	0.127

[a] Determined by ^{1}H NMR spectroscopy using the signals at 4.20 ppm and 2.10 ppm. [b] Determined by end-group analysis from ^{1}H NMR spectroscopy. [c] From SEC based on poly(methyl methacrylate) standards. [d] By differential refractometry.

back filled with nitrogen, sealed and placed in a pre-heated oil bath at 70 °C. After 7 hours the polymerization was quenched by liquid nitrogen, dioxane removed *in vacuo* and the resultant polymer diluted with H$_2$O. The solution was transferred to a dialysis membrane tube with the appropriate molecular weight cut-off (MWCO 3.5 kDa) and dialyzed against 18.2 MΩ cm water (1.5 L) with 3 water changes. Lyophilization resulted in a pink copolymer which is further extended in the next synthesis step. ^{1}H NMR (400 MHz, CDCl$_3$): δ (ppm) 7.85 (d, J = 8.1 Hz, 1H Ar end group), 7.55 (t, J = 7.4 Hz, 2H end group), 7.41 (t, J = 8.1 Hz, 2H, end group), 4.20 (br t, 2H, OCH_2CH$_2$N), 2.50 (br s, 2H, OCH$_2$CH_2N), 2.30 (br t, 4H, OCH$_2$CH$_2$N(CH_2)$_2$(CH$_3$)$_2$), 2.10 (br s, 6H, OCH$_2$CH$_2$N(CH_3)$_2$), 1.94 (s, 6H, end group), 1.10 (br t, 6H, OCH$_2$CH$_2$N(CH$_2$)$_2$(CH_3)$_2$), 1.00–2.00 (br m, backbone) (See Table 1 for molecular weight data).

General procedure for chain extension of the copolymers with DMAEMA

Macro chain transfer agent (Macro-CTA) (1.0 eq.), AIBN (0.2 eq.) and DMAEMA (40 eq.) were dissolved in DMF (1 : 1 volume compared to the monomer) and were added to a dry ampoule containing a stirrer bar. The solution was degassed using at least 3 freeze–pump–thaw cycles, back filled with nitrogen, sealed and placed in a pre-heated oil bath at 70 °C. After 7 hours the polymerization was quenched by liquid nitrogen, DMF was removed *in vacuo* and the resultant polymer diluted with H$_2$O and transferred to a dialysis membrane tube with the appropriate molecular weight cut off (MWCO 6–8 kDa) and dialyzed against 18.2 MΩ cm water (1.5 L) with 3 water changes. Lyophilization resulted in a pink polymer. ^{1}H NMR (400 MHz, CDCl$_3$): δ (ppm) 7.85 (d, J = 8.1 Hz, 1H end group), 7.55 (t, J = 7.4 Hz, 2H end group), 7.41 (t, J = 8.1 Hz, 2H, end group), 4.20 (br t, 2H, OCH_2CH$_2$N), 2.50 (br s, 2H, OCH$_2$CH_2N), 2.30 (br t, 4H, OCH$_2$CH$_2$N(CH_2)$_2$(CH$_3$)$_2$), 2.10 (br s, 6H, OCH$_2$CH$_2$N(CH_3)$_2$), 1.94 (s, 6H, end group), 1.10 (br t, 6H, OCH$_2$CH$_2$N(CH$_2$)$_2$(CH_3)$_2$), 1.00–2.00 (br m, backbone) (see Table 1 for molecular weight data).

Reactivity ratios of DMAEMA and DEAEMA

DMAEMA and DEAEMA at different molar ratios, CPDB and AIBN were dissolved in 1,4-dioxane. The ratio of [monomers] : [CTA] : [AIBN] was 40 : 1 : 0.2, the solution was degassed using at least 3 freeze–pump–thaw cycles, back-filled with nitrogen,

sealed and placed in a pre-heated oil bath at 70 °C. The conversion was kept below 10% and the reaction was quenched by liquid nitrogen. Aliquots were taken and characterized by ^{1}H NMR spectroscopy in CDCl$_3$.

^{1}H nuclear magnetic resonance (NMR) spectroscopy

^{1}H NMR spectra were recorded on a Bruker DPX-400 spectrometer in CDCl$_3$. Chemical shifts are given in ppm downfield from TMS.

Size exclusion chromatography

Size exclusion chromatography (SEC) measurements were performed with HPLC grade solvents (Fisher), dimethylformamide (DMF) with 1.06 g L^{-1} of LiCl at 40 °C as an eluent at a flow rate of 1 mL min^{-1}, on a set of two PLgel 5 μm Mixed-D columns, and one guard column. The molecular weights of the synthesized polymers were calculated relative to poly(methyl methacrylate) (PMMA) standards from refractive index traces.

Potentiometric titration

Potentiometric titration was performed at room temperature with an automatic titrator (Mettler Toledo G20) controlled by LabX software. 40 mL of solution (approximately 2.3×10^{-4} M) was used for each potentiometric titration experiment. The polymers were first dissolved at $\alpha = 1$ with 1.1 excess of 1 M HCl and then back-titrated with 0.1 M NaOH. We define α as the degree of ionization following eqn (1),

$$\alpha = \frac{[\text{NR}_2\text{H}^+\text{Cl}^-]}{[\text{NR}_2]_{\text{total}}} \tag{1}$$

where complete protonation of the amine units corresponds to $\alpha = 1$ and complete deprotonation of amine units to $\alpha = 0$.

The addition of NaOH 0.1 M titrant was added at volume increments of 5–50 μL and spaced with 180 s intervals. From the raw titration data the total amount of titratable amine units was calculated.[27] Therefore, the change of pH could be plotted as a function of the degree of ionization, α.

Refractive index increment

The specific refractive index increment (dn/dC) of the polymers were measured on a refractometer (Bischoff RI detector) operating at a wavelength of 632 nm.

Sample preparation

Two methods for the preparation of the solutions were used in the following. Method 1 consisted of diluting polymer stock solutions that were prepared at 20 g L^{-1} by dispersing the polymer in 18.2 MΩ CM water containing the appropriate amount of HCl to reach $\alpha = 1$. After one night of stirring α was lowered with the required amount of 1 M NaOH and the solutions were stirred again overnight, after which time the NaCl concentration was adjusted to 0.1 M by the addition of 4 M NaCl. The solutions were further stirred overnight before use. Samples at lower concentrations were subsequently diluted

with 0.1 M NaCl to reach the desired concentrations (10 g L^{-1}– 0.5 g L^{-1}).

For reversibility tests method 2 was used. Method 2 consisted of making a polymer solution at $\alpha = 1$ as for method 1 at a concentration of 2.5 g L^{-1}. Subsequently this solution was split in two. One half of the solution was brought to lower α values by the addition of 1 M NaOH (this will be referred to as Pathway A). The second half was first brought to $\alpha = 0$ from the addition of 1 M NaOH, knowing the chemical structure of the polymers and considering that all units are ionizable as verified by potentiometric titration. Then α values were raised by the addition of 1 M HCl (referred to as Pathway B). Each change in α was spaced by at least one night of stirring.

Laser light scattering

Measurements were performed at angles of observation ranging from 20° up to 150° with an ALV CGS3 setup operating at $\lambda_0 = 632$ nm and at 20 ± 1 °C. Data were collected in duplicate with 240 s run times. Calibration was achieved with filtered toluene and the background was measured with filtered solvent (NaCl 0.1 M).

Dynamic light scattering (DLS)

The intensity autocorrelation functions $g_2(t)$ obtained from dynamic light scattering were related to $g_1(t)$ (the normalized electric field autocorrelation functions) via the so-called Siegert relation. Then $g_1(t)$ was analyzed in terms of a continuous distribution of relaxation times (eqn (2)) using the REPES routine[28] without assuming a specific mathematical shape for the distribution of the relaxation times ($A(\tau)$).

$$g_1(t) = \int_0^\infty A(\tau)\exp(-t/\tau)\mathrm{d}\tau \tag{2}$$

The apparent diffusion coefficient D was calculated from (eqn (3)) given that the average relaxation rates Γ of the scatterers were q^2 dependent, where q is the scattering vector given by $q = (4\pi n/\lambda_0)\sin(\theta/2)$ with θ the angle of observation and $n = 1.333$ the refractive index of the solvent (water).

$$D = \Gamma/q^2 \tag{3}$$

Its concentration dependence is given by $D = D_0(1 + k_{\text{D}}C)$ where k_{D} is the dynamic second virial coefficient and D_0 the diffusion coefficient used for computing the hydrodynamic radius (R_{h}) of the scatterers according to the Stokes–Einstein equation (eqn (4))

$$D_0 = \frac{kT}{6\pi\eta R_{\text{h}}} \tag{4}$$

with η the solvent viscosity, k the Boltzmann's constant and T the absolute temperature. Values of R_{h} given in the following are then obtained after extrapolation to zero concentration.

Static light scattering (SLS)

The Rayleigh ratio of the solutions have been measured using toluene as a reference according to: $R_\theta = (I_{\text{solution}}(\theta) - I_{\text{solvent}}(\theta))/$

$I_{\text{toluene}}(\theta) R_{\text{tol}}$ where I_i represents the intensity scattered by species $_i$ and R_{tol} is the Rayleigh ratio of the reference. In dilute solutions if $R_g q < 1$ where R_g is the radius of gyration, the q and concentration dependence of R_θ is given by (eqn (5)).

$$\frac{KC}{R_\theta} = \left(\frac{1}{M_w} + 2A_{2C}\right)\left(1 + \frac{q^2 R_g{}^2}{3}\right) \tag{5}$$

where A_2 is the second virial coefficient and M_w the weight average molecular weight. K is an optical constant given by (eqn (6)):

$$K = \frac{4\pi^2 n_o{}^2}{\lambda^4 N_A}\left(\frac{dn}{dC}\right)^2 \tag{6}$$

where $n_o = 1.496$ is the refractive index of the reference liquid (toluene), dn/dC is the specific refractive index increment determined by differential refractometry (see Table 1) and N_A is Avogadro's number. Values of M_w are then obtained after extrapolation to zero concentration and zero angle and used to derive the aggregation number of the micellar aggregates $N_{\text{agg}} = M_w/M_{w,\text{unimers}}$. For spherical morphologies, it is possible to deduce the core radius, R_c, from the aggregation number, using eqn (7) assuming the core block is dehydrated and the density matches that of the bulk value, ρ.[29]

$$\frac{4\rho R_c{}^3}{3} = N_{\text{agg}} \frac{M_{w\ \text{Hydrophobic block}}}{N_A} \tag{7}$$

When in some cases two modes of relaxation were observed by DLS measurements, R_θ was described as the sum of two contributions according to (eqn (8)).

$$R_\theta = R_{\theta f} + R_{\theta s} \tag{8}$$

where f and s stand respectively for fast and slow and using (eqn (9)):

$$R_{\theta f}(q) = \frac{A_f(q)}{(A_f(q) + A_s(q))} R_\theta \tag{9}$$

where A_f and A_s are the relative amplitudes of the fast and slow modes obtained by DLS. The slow mode of relaxation when observed can be attributed to spurious aggregates with a negligible weight fraction but larger scattering intensity.[30–32]

Small angle X-ray scattering (SAXS)

Measurements were performed at the Australian Synchrotron facility at a photon energy of 11 keV. The samples in solutions of 0.1 M NaCl were collected at a sample to detector distance of 3.252 m to give a q range of 0.004 to 0.2 Å^{-1}. The scattering from a blank (aqueous solution of NaCl 0.1 M) was measured in the same location as the sample collection and was subtracted for each measurement. Data were normalized for total transmitted flux using a quantitative beamstop detector and absolute scaled using water as an absolute intensity standard. The two-dimensional isotropic SAXS images were converted into one-dimensional SAXS scattered intensity profiles ($I(q)$ versus q) by circular averaging. The functions used for the fitting from NCNR package[33] were "Guinier-Porod",[34,35] "Core–

Shell"[35] and "Debye".[36] Scattering length densities (SLD) were calculated using the "Scattering Length Density Calculator"[37] provided by the NIST Center for Neutron Research.

Cryogenic transmission electron microscopy samples (cryo-TEM)

3.5 µL of sample was added to freshly glow discharged Quanti-foil R2/2 TEM grids. The grids were blotted with filter paper under high humidity to create thin films and rapidly plunged into liquid ethane. The grids were transferred to the microscope under liquid nitrogen and kept at <−175 °C while imaging.

Results and discussion

Synthesis and molecular characterization of the diblock copolymers

The polymer synthesis must be controlled to allow for similar block lengths, to allow us to understand the effect of composition for the responsive block, whilst being tolerant to the responsive functionality. Therefore, reversible addition fragmentation chain transfer, RAFT, polymerization was selected.[6,38,39] Various macro-CTAs were synthesized by RAFT (Scheme 1) which consisted of copolymers of DMAEMA and DEAEMA with various amounts of each comonomer. To confirm the microstructure of the macro-CTAs, reactivity ratios were calculated using a non-linear least-squares fitting method, developed by van Herk.[40] Both F_1 (mol fraction of DMAEMA in the copolymer) and f_1 (mol fraction of DMAEMA in the monomer feed) values were used to determine the reactivity ratio of the monomers shown in Scheme 1. The generated values for r_1 and r_2 were as follows; DMAEMA, $r_1 = 1.140$ and DEAEMA, $r_2 = 0.824$, leading to $r_1 r_2 = 0.939$ (ESI, Fig. S1†),[41] which shows a near ideal copolymerization. The macro-CTA copolymers can therefore be considered as statistical copolymers. The macro-CTA copolymers were chain-extended with DMAEMA, Scheme 1, which gave diblock copolymers with a controlled incorporation of responsive monomer, known molecular weights and low dispersities as summarized in Table 1. Note that similar block lengths were targeted for all polymers.

Ionization behavior

For diblock copolyelectrolytes it has been concluded that ionization behavior is different to that of simple homopolyelectrolytes.[27] Moreover, for the system studied herein both monomers in both blocks can be ionized. Therefore, we explored how the microstructure of the diblock copolymers
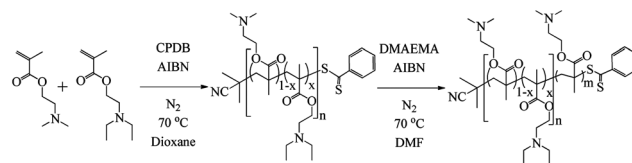
Scheme 1 Copolymerization of DMAEMA and DEAEMA and chain extension with DMAEMA *via* RAFT polymerization.
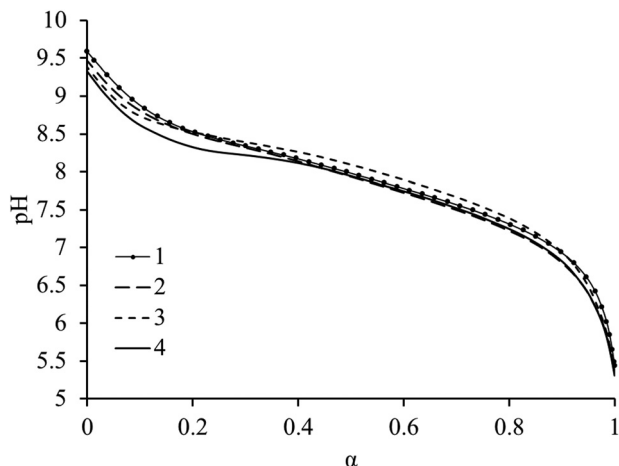
Fig. 1 Evolution of ionization degree α, with pH for the diblock copolymers, **1–4**.

Fig. 2 Evolution of N_{agg} with increasing (pathway B) or decreasing (pathway A) the ionization for **2**, **3** and **4** at 2.5 g L^{-1} 0.1 M NaCl solution.

altered their ionization behavior *via* potentiometric titration experiments. Diblock copolymers were soluble in water with a 1.1 stoichiometric excess of 1 M HCl with respect to ionizable units. Subsequently these solutions were back titrated with 0.1 M NaOH to allow for the determination of the evolution of ionization degree, α, with respect to pH.[27,42] Comparing the ionization behavior of the diblock copolymers (from **1** to **4**) we observe the pH range in which ionization occurs (Fig. 1). It was observed that ionization of all the amine units can occur, regardless of their location in the polymer chain whether they are in a core or coronal forming block as ionization may be facilitated by the presence of NaCl salt which can screen charges along the polymer chain. Additionally we note that although the copolymer composition differs greatly between all polymers, ionization behavior does not. This indicates that the relationship of composition, that is the incorporation of DEAEMA, to ionization is relatively weak for this series of diblock copolymers despite being structurally different to homopolyelectrolytes.

Aqueous solution properties: pathway dependence on the self-assembly

Although a system may reorganize after a change in pH this does not mean the change is reversible or that the system is in equilibrium. As shown by both Bendejacq[15] and Jacquin[43] respectively with poly(styrene)-*block*-poly(acrylic acid) and poly-(*n*-butyl acrylate)-*block*-poly(acrylic acid) diblock copolymers, irreversible morphological changes of the aggregates can occur upon variation of the degree of ionization of the polyelectrolyte. Therefore, to establish whether the pH-sensitivity is reversible or not is highly relevant in being able to assess the relationship of copolymer composition with aggregation behavior. Indeed, non-reversible pH-sensitivity implies that the aggregates are out-of-equilibrium "frozen" structures whose characteristics strongly depend on the method used to disperse them in solution, which will lead to an array of different macro scale properties for one polymer system.[4,19] To assess if
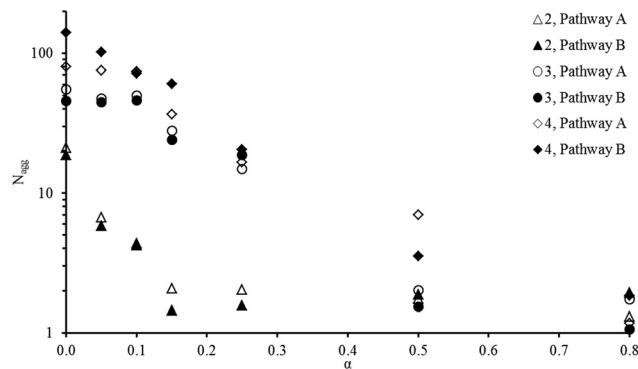
irreversible reorganization had occurred, initial reversibility tests using LLS (see the Experimental section for details of sample preparation, method 2 (ESI, Fig. S2†)) were undertaken. Briefly, method 2 consists of reaching a given ionization degree either from a higher (pathway A) or a lower (pathway B) ionization degree.

As can be seen in Fig. 2, N_{agg} varies both upon increasing or decreasing α (respectively through decreasing or increasing the pH of the solution) and varies with the copolymer composition. Although pathways A and B do not lead exactly to the same N_{agg} (Fig. 2), especially at the lowest α values for polymer **4** (91% DEAEMA), the differences between the two pathways remain small. These results confirm that the reorganization of the system observed as a function of the ionization degree (respective of the pH) is reversible. Nevertheless, this behavior is highly interesting from an applicative point of view as the structures formed show no pathway dependence. Moreover, it is possible to alter the chemical structure to the target application such as tumour targeting[44] and polymer delivery agents,[45] where decisive structure and response is needed, by copolymerizing two types of monomers to form a moderately hydrophobic core block. Furthermore, the reversible nature of these polymers suggests that the hydrophobic blocks exchange in a dynamic way between hydrophobic cores thus indicating the system is not frozen and is under thermodynamic control. Further analysis such as rheology,[12] time-resolved SANS[3,17] or fluorescence[46,47] could be used to probe quantitatively the exchange dynamics.

Aqueous solution properties: influence of DEAEMA incorporation

While this system is believed to be under thermodynamic control with no pathway dependence, in the following section all polymer solutions were prepared using method 1 as described in the Experimental section. For all polymers a second slow mode of relaxation is observed by DLS in some instances which can be attributed to spurious aggregates with a negligible weight fraction but larger scattering intensity.[30–32] However, these only occur at high degrees of ionization which is when the scattering of the polymer aggregates is relatively low (ESI, Fig. S7†). Fig. 3a and b represent respectively the evol-
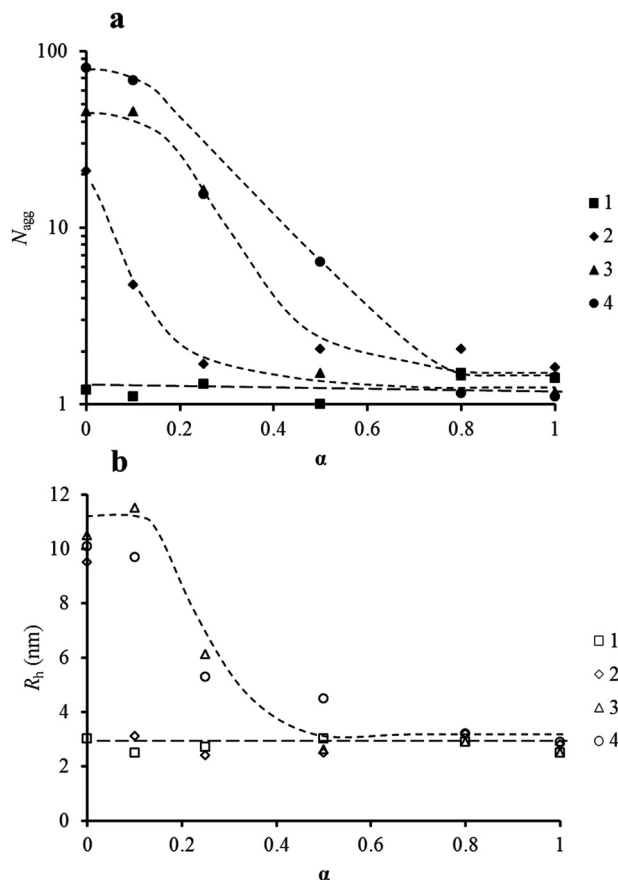
Fig. 3 (a) Evolutions of N_{agg} with α for polymers **1**, **2**, **3** and **4**. (b) Evolutions of R_h with α for polymers **1**, **2**, **3** and **4**. Values of N_{agg} and R_h given are obtained by extrapolation to zero concentration. Lines are included as a guide for the reader.

ution of the aggregation number and the hydrodynamic radius of the polymers with the ionization degree as measured by light scattering. For polymer **1** (that is the polymer with the lowest incorporation of hydrophobic monomer incorporated within the hydrophobic block), we observe no change in both R_h and N_{agg} within experimental error irrespective of α. As N_{agg} remains equal to 1, we can conclude that polymer **1** does not aggregate.

Moreover, the R_h values can then be used to serve as a reference for unimers (unaggregated chains) for other compositions since they exhibit the same block length. In contrast to **1**, all experiments indicate that both R_h and N_{agg} increase significantly from $\alpha = 1$ to $\alpha = 0$ for polymers **2–4**. These polymers exhibit pH-sensitive aggregation behavior as the large changes in α are produced from slight changes in pH as observed in Fig. 1. Interestingly, the ionization degree at which aggregation starts is shifted toward higher values as the content of hydrophobic monomer (DEAEMA) within the statistical hydrophobic block increases. Polymer **2** self-assembles only at low ionization values, below 0.1. Moreover, **2** does not reach a plateau or limit for its aggregation in the ionization region studied. For polymers **3** and **4** similar behavior is detected, where a gradual

increase in R_h and N_{agg} with decreasing α was observed. Both **3** and **4** reach a plateau region in their aggregation behavior, but the aggregation of **4** starts below 0.8, whereas it must be lower than 0.5 for polymer **3**.

The relationship between the chemical composition of the polymers and the α-sensitivity of their aggregation may seem expected but polymer aggregation is a result of both kinetic and thermodynamic factors, consequently many polymers will not follow such aggregation trends. This subtle balance between more charges along the polymer backbone (which gave increased hydrophilicity to the polymer from electrostatic repulsions from charged units) *versus* the aggregation of the hydrophobic DEAEMA units from tailoring the chemical structure allows easy tuning of aggregation over a wide range. Specifically, as the DEAEMA incorporation is reduced the effective hydrophobicity of the polymer is reduced. This in turn leads to a lower α value being needed for the polymers to aggregate. Indeed, using the potentiometric titration experiments described above, the evolution of the aggregation number and hydrodynamic radius of the polymer assemblies could be plotted as a function of pH rather than as a function of α (Fig. 4). Fig. 4 reveals the wide pH range where aggregation occurs can be controlled by tuning the composition of the
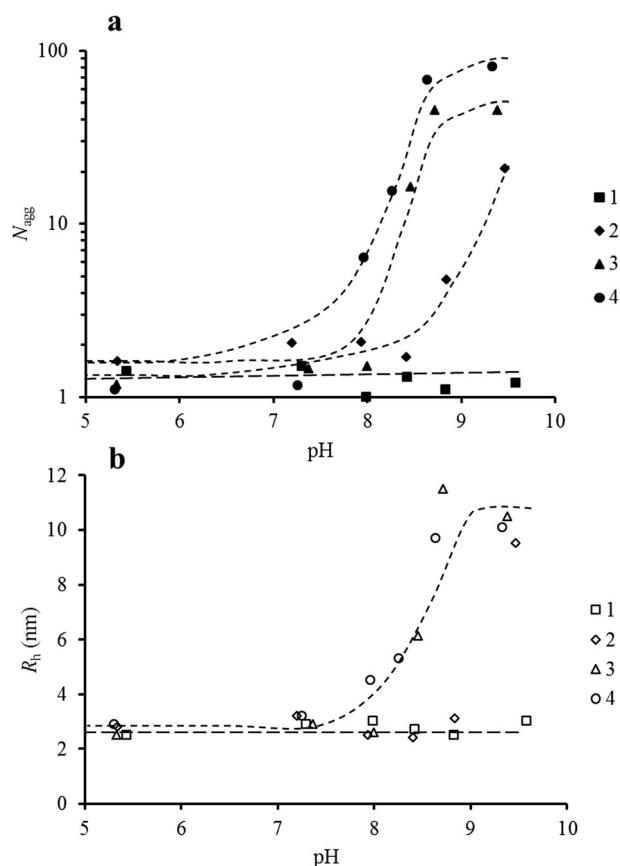

Fig. 4 (a) Evolutions of N_{agg} with pH for polymers **1**, **2**, **3** and **4**. (b) Evolutions of R_h with pH for polymers **1**, **2**, **3** and **4**. Values of N_{agg} and R_h given are obtained by extrapolation to zero concentration. Lines are included as a guide for the reader.

View Article Online

statistical hydrophobic block alone offering great potential over conventional homopolymeric diblock copolymers.

The values of N_{agg} and R_h are compatible with a spherical core shell micelle morphology, involving a dense core surrounded by a partially extended corona (ESI, Tables S2–5 and for calculations, Fig. S9†) for all the polymer micelles.[45–47] This assembly of polymers into a spherical morphology can be corroborated with cryo-TEM images for polymers **2**, **3** and **4** (ESI, Fig. S9†). To further explore this spherical core-shell micelle morphology **3** was further examined with SAXS, here the DEAEMA incorporation is constant but the ionization degree was varied. Additionally with SAXS the core of these particles can be probed (ESI, Table S5 and Fig. S8†), however, we do observe a larger core from SAXS in comparison to a theoretical value obtained from SLS. This difference in core sizes can be attributed to the contrast difference between the core and corona; due to the similarities between the two the corona is partially seen. Nevertheless, the trends with changing α are identical to those observed from LLS, an increase in α causes the micelles to disassemble and smaller N_{agg} and micelle radius values are obtained. Therefore SAXS confirms the highly pH sensitive behavior of these diblock copolymers with a copolymer associating block (ESI, further analysis†).

Since all polymers have similar block lengths N_{agg} and R_h at $\alpha = 0$ can be represented as a function of DEAEMA incorporation in the core for the polymers which self-assemble (Fig. 5). It can be shown that the N_{agg} value is independent of R_h within experimental error. Indeed the R_h values show a change of <1 nm across an incorporation range of 25%, whilst the N_{agg} values differ up to approximately 4 times. Fig. 5 highlights the strong relationship between the core hydrophobicity and the nature of the aggregates formed, highlighting that even low incorporations of monomers with different solvophobicity into the core may have significant impact on the final structure formed. This behavior is especially vital in self-assembled nanostructures in catalysis[48] and nanomedicine,[49] where moderating the cores of micelles has been shown to vastly change performance in nanostructures.[50]
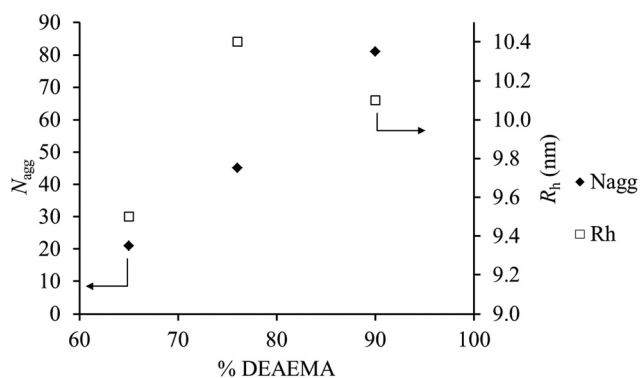
Conclusions

A series of P(DEAEMA-co-DMAEMA)-b-PDMAEMA diblock copolymers have been synthesized with varying degrees of DEAEMA in the core block. In aqueous media, below a given ionization degree, the polymers self-assemble into pH sensitive star like micelles, similar to the behavior of its analogous PDEAEMA-b-PDMAEMA diblock copolymer. However, contrary to what was observed for the analogous diblock, the pH region of aggregation for these P(DEAEMA-co-DMAEMA)-b-PDMAEMA diblock copolymers can be shifted by modifying the composition of the statistical hydrophobic block. In comparison to the analogous PDEAEMA-b-PDMAEMA diblock copolymer by decreasing the ionization the aggregation of the polymers shows an exponential relationship to the aggregation number. The apparent aggregation number was shown to change reversibly for the micelles irrespective of the preparation pathway, which indicates that there is reorganization of the system. This makes it suitable from an applicative point of view, whereby a single polymer can be used to access a wide range of aggregates in a desired pH region. Moreover the aggregation number of these star-like micelles can be increased up to 4 times by varying the incorporation of DEAEMA (from 65% to 91%) in the core block, whilst maintaining equal block lengths and micelle sizes in solution. The ability to selectively tune the aggregation behavior of responsive polymers from subtle differences in polymer composition stresses the great sensitivity and ability to decisively tune diblock copolymer assemblies.

Acknowledgements

Fig. 5 Effect of the DEAEMA loading on the N_{agg} and R_h for polymers **2**, **3** and **4** at $\alpha = 0$. Values of N_{agg} and R_h given are obtained by extrapolation to zero concentration.

Notes and references

1 I. W. Hamley, *The Physics of Block Copolymers*, OUP Oxford, 1998.
2 I. W. Hamley, *Block Copolymers in Solution: Fundamentals and Applications*, Wiley, 2005.
3 S.-H. Choi, T. P. Lodge and F. S. Bates, *Phys. Rev. Lett.*, 2010, **104**, 047802.
4 S. Y. Choi, F. S. Bates and T. P. Lodge, *J. Phys. Chem. B*, 2009, **113**, 13840.
5 N. Petzetakis, D. Walker, A. P. Dove and R. K. O'Reilly, *Soft Matter*, 2012, **8**, 7408.

6 P. Cotanda, D. B. Wright, M. Tyler and R. K. O'Reilly, *J. Polym. Sci., Part A: Polym. Chem.*, 2013, **51**, 3333.

7 J.-F. Lutz, *J. Polym. Sci., Part A: Polym. Chem.*, 2008, **46**, 3459.

8 J.-F. Lutz, Ö. Akdemir and A. Hoth, *J. Am. Chem. Soc.*, 2006, **128**, 13046.

9 A. Shedge, O. Colombani, T. Nicolai and C. Chassenieux, *Macromolecules*, 2014, **47**, 2439.

10 C. Charbonneau, M. M. D. Lima, C. Chassenieux, O. Colombani and T. Nicolai, *Phys. Chem. Chem. Phys.*, 2013, **15**, 3955.

11 F. Dutertre, O. Boyron, B. Charleux, C. Chassenieux and O. Colombani, *Macromol. Rapid Commun.*, 2012, **33**, 753.

12 C. Charbonneau, C. Chassenieux, O. Colombani and T. Nicolai, *Macromolecules*, 2011, **44**, 4487.

13 E. Lejeune, C. Chassenieux and O. Colombani, *Prog. Colloid Polym. Sci.*, 2011, **138**, 7.

14 E. Lejeune, M. Drechsler, J. Jestin, A. H. E. Muller, C. Chassenieux and O. Colombani, *Macromolecules*, 2010, **43**, 2667.

15 D. D. Bendejacq and V. Ponsinet, *J. Phys. Chem. B*, 2008, **112**, 7996.

16 D. D. Bendejacq, V. Ponsinet and M. Joanicot, *Langmuir*, 2005, **21**, 1712.

17 R. Lund, L. Willner, D. Richter and E. E. Dormidontova, *Macromolecules*, 2006, **39**, 4566.

18 T. Nicolai, O. Colombani and C. Chassenieux, *Soft Matter*, 2010, **6**, 3111.

19 R. C. Hayward and D. J. Pochan, *Macromolecules*, 2010, **43**, 3577.

20 J. Hu, G. Zhang, Z. Ge and S. Liu, *Prog. Polym. Sci.*, 2014, **39**, 1096.

21 J. Hu and S. Liu, *Macromolecules*, 2010, **43**, 8315.

22 X. Jiang, Z. Ge, J. Xu, H. Liu and S. Liu, *Biomacromolecules*, 2007, **8**, 3184.

23 A. S. Lee, V. Bütün, M. Vamvakaki, S. P. Armes, J. A. Pople and A. P. Gast, *Macromolecules*, 2002, **35**, 8540.

24 A. S. Lee, A. P. Gast, V. Butun and S. P. Armes, *Macromolecules*, 1999, **32**, 4302.

25 H. Lee, S. H. Son, R. Sharma and Y.-Y. Won, *J. Phys. Chem. B*, 2011, **115**, 844.

26 P. van de Wetering, N. J. Zuidam, M. J. van Steenbergen, O. van der Houwen, W. J. M. Underberg and W. E. Hennink, *Macromolecules*, 1998, **31**, 8063.

27 O. Colombani, E. Lejeune, C. Charbonneau, C. Chassenieux and T. Nicolai, *J. Phys. Chem. B*, 2012, **116**, 7560.

28 J. Jakes, *Collect. Czech. Chem. Commun.*, 1995, **60**, 1781.

29 J. P. Patterson, M. P. Robin, C. Chassenieux, O. Colombani and R. K. O'Reilly, *Chem. Soc. Rev.*, 2014, **43**, 2412.

30 C. Chassenieux, T. Nicolai and D. Durand, *Macromolecules*, 1997, **30**, 4952.

31 M. Sedlak, *J. Chem. Phys.*, 1997, **107**, 10805.

32 M. Sedlak, *J. Chem. Phys.*, 1997, **107**, 10799.

33 S. Kline, *J. Appl. Crystallogr.*, 2006, **39**, 895.

34 O. Glatter and O. Kratky, *Small-Angle X-Ray Scattering*, Academic Press, 1982.

35 A. Guinier and G. Fournet, *Small-angle scattering of X-rays*, John Wiley & Sons, New York, 1955.

36 R.-J. Roe, *Methods of X-ray and Neutron Scattering in Polymer Science*, Oxford University Press, New York, 2000.

37 NIST SLD calculator http://www.ncnr.nist.gov/resources/sldcalc.html.

38 D. J. Keddie, *Chem. Soc. Rev.*, 2014, **43**, 496.

39 G. Moad, E. Rizzardo and S. Thang, *Macromolecules*, 1998, **31**, 5559.

40 A. M. Van Herk and T. Dröge, *Macromol. Theory Simul.*, 1997, **6**, 1263.

41 P. J. Flory, *Principles of Polymer Chemistry*, Cornell Univ Pr, 1953.

42 M. S. Picidn, *Makromol. Chem.*, 1985, **186**, 111.

43 M. Jacquin, P. Muller, R. Talingting-Pabalan, H. Cottet, J. F. Berret, T. Futterer and O. Theodoly, *J. Colloid Interface Sci.*, 2007, **316**, 897.

44 Y. Wang, K. Zhou, G. Huang, C. Hensley, X. Huang, X. Ma, T. Zhao, B. D. Sumer, R. J. DeBerardinis and J. Gao, *Nat. Mater.*, 2014, **13**, 204.

45 R. Haag, *Angew. Chem., Int. Ed.*, 2004, **43**, 278.

46 J. van Stam, S. Creutz, F. C. De Schryver and R. Jerome, *Macromolecules*, 2000, **33**, 6388.

47 S. Creutz, J. van Stam, F. C. De Schryver and R. Jerome, *Macromolecules*, 1998, **31**, 681.

48 A. Lu and R. K. O'Reilly, *Curr. Opin. Biotechnol.*, 2013, **24**, 639.

49 J. H. Park, S. Lee, J.-H. Kim, K. Park, K. Kim and I. C. Kwon, *Prog. Polym. Sci.*, 2008, **33**, 113.

50 A. Lu, D. Moatsou, D. A. Longbottom and R. K. O'Reilly, *Chem. Sci.*, 2013, **4**, 965.

Supporting Information

Tuning the aggregation behaviour of pH responsive micelles by copolymerization

Daniel B. Wright, [a] Joseph P. Patterson, [a] Anaïs Pitto-Barry, [a] Pepa Cotanda, [a] Christophe Chassenieux, [b]*

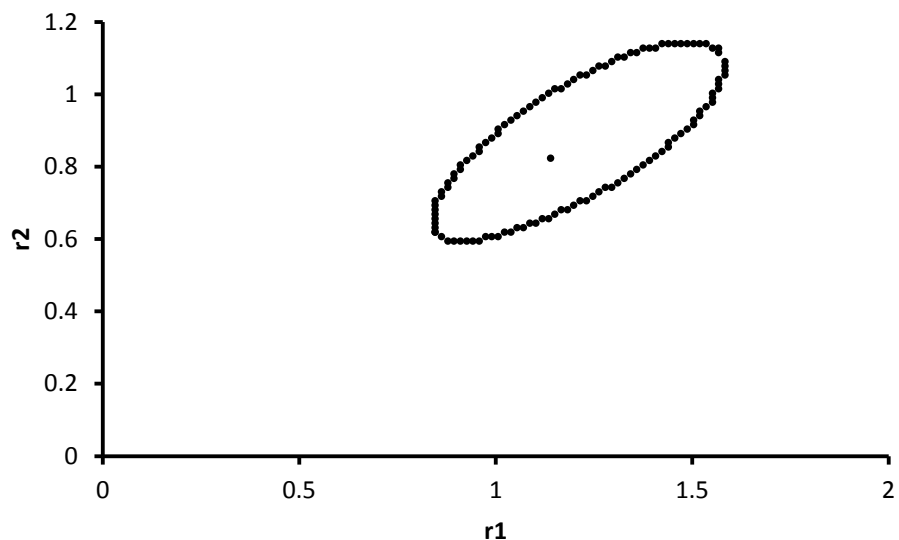Olivier Colombani, [b]* and Rachel K. O'Reilly [a]*

Figure S1. 95% joint confidence intervals of the r_1 and r_2 values for the DMAEMA/DEAEMA copolymerization determined using a nonlinear least-squares fitting method, developed by van Herk. [1]

Table S1. f1 and F1 values for the copolymerization of DMAEMA(f1) and DEAEMA(f2).

Experiment	Mol fraction in initial feed (f1)	Mol fraction in copolymer (F1)
1	0.09	0.09
2	0.25	0.32
3	0.32	0.35
4	0.37	0.41
5	0.54	0.55
6	0.60	0.63
7	0.71	0.76
8	0.83	0.86

A stock solution of polymer at α = 1 was split in two.

For one half of the solution the α value was **decreased** by additions of NaOH.

Pathway A

Start at α = 1

Addition of NaOH → α = 0

Addition of NaOH → α = 0

Addition of HCl → α = 1

Addition of NaOH → α = 0

The second half was brought to α = 0 and subsequently **increased** by additions of HCl.
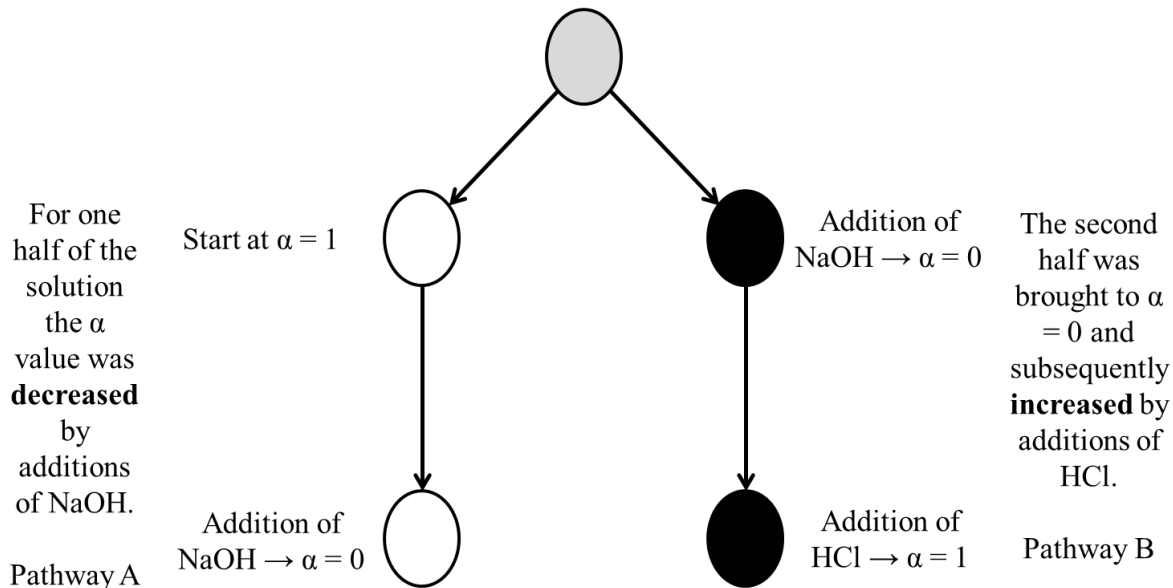
Pathway B

Figure S2. Schematic showing the 2 pathways (A and B) used for the reversibility testing in sample preparation Method 2.

Table S2. Effect of ionization on the characteristics of polymer **1**.

α	M_w (kg.mol^{-1}) [a]	N_{agg} [a]	R_h (nm) [b]
0	13	1.2	3.0
0.1	12	1.1	2.5
0.25	13	1.3	2.7
0.5	12	1	3.0
0.8	13	1.5	2.9
1	13	1.4	2.5

[a] Determined by SLS, M_w is the weight-average molecular weight of the scatterers. [b] Determined from DLS.

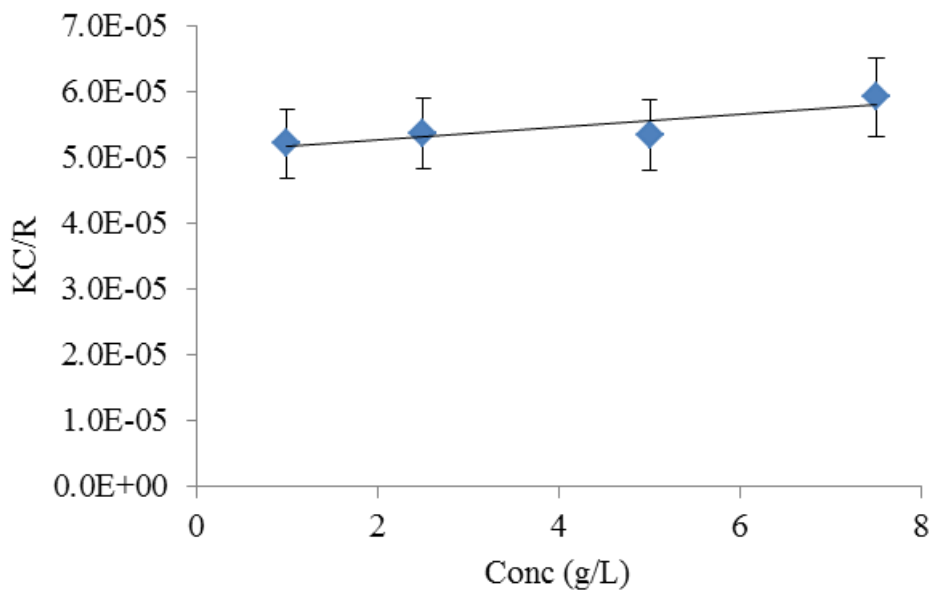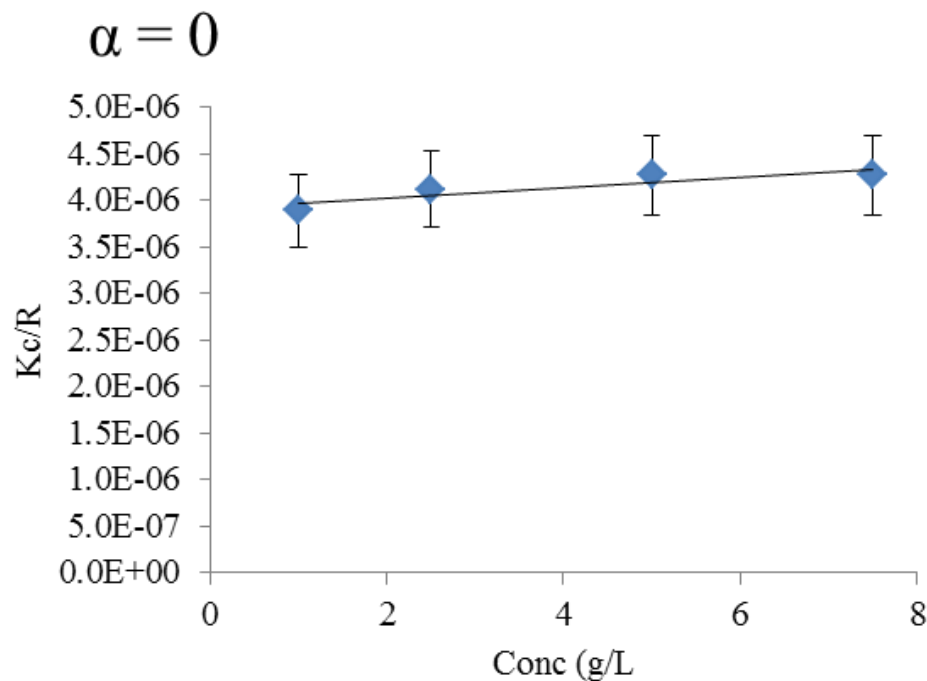**Figure S3.** Example SLS data plotted as Kc/RΘ versus concentration for **1** at α = 0.

Table S3. Effect of ionization on the characteristics of polymer **2**.

α	M_w (kg.mol^{-1}) [a]	N_{agg} [a]	R_h [b] (nm)	R_c [c] (nm)	Corona Stretching (%)[d]
0	256	21	9.5	3.9	64
0.1	58	5	3.1	e	e
0.25	21	2	2.4	e	e
0.5	25	2	2.5	e	e
0.8	25	2	3.2	e	e
1	20	2	2.8	e	e

[a] From SLS, M_w is the weight-average molecular weight of the scatterers. [b] Determined from DLS. [c] Calculated from equation 7 assuming a core density of 1. [d] $(R_{hDLS}-R_{cSLS})/L_{contour,DMAEMA}$. [e]For polymers above α = 0 the model of "core-corona" is no longer applicable.

Figure S4. Example SLS data plotted as Kc/RΘ versus concentration for **3** at α = 0.

Table S4. Effect of ionization on the characteristics of polymer 3.

α	M_w (kg.mol^{-1})[a]	N_{agg}[a]	R_h[b](nm)	R_g^c(nm)	R_c^c(nm)	R_c^f(nm)	Corona Stretching (%)[h]
0	556	46	10.5	8.5[d]	4.9	4.6	70
0.1	556	46	11.5	-	-	4.6	81
0.25	200	16	6.1	7.5[d]	5.3	3.2	34
0.5	18	1	2.6	-	-	h	h
0.8	18	1	2.9	3.7[e]	-	h	h
1	14	1	2.5	3.5[e]	-	h	h

[a] From SLS, M_w is the weight-average molecular weight of the scatterers. [b] Determined from DLS. [c] From SAXS at a concentrations of 2.5 gL^{-1} using method1. [d] Determined with the Guinier-Porod model. [e] Determined with the Debye model. [f] Calculated from equation 7 assuming a core density of 1. [g] (R_{hDLS}-R_{cSLS})/$L_{contour,DMAEMA}$. [h]For polymers above $\alpha = 0.25$ the model of "core-corona" is no longer applicable.

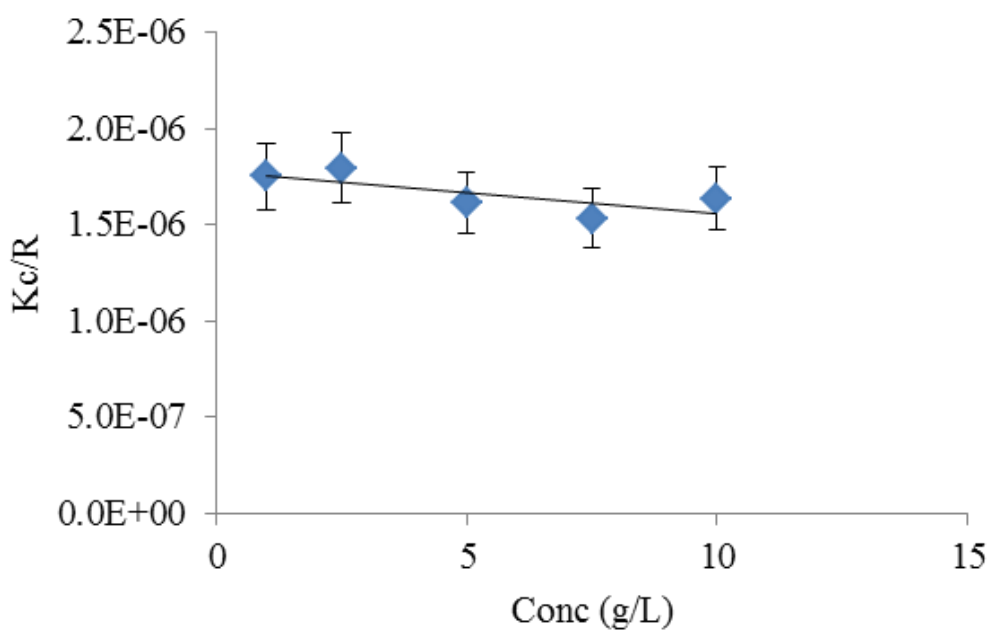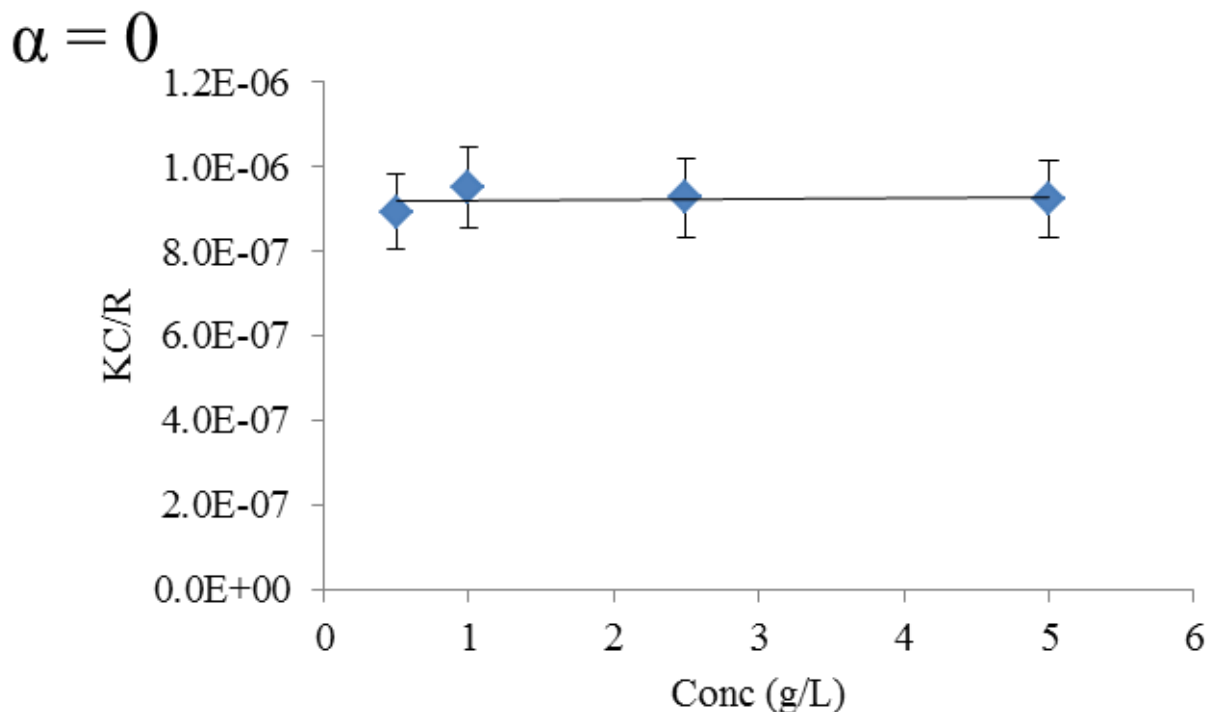**Figure S5.** Example SLS data plotted as Kc/RΘ versus concentration for **3** at α = 0.

Table S5. Effect of ionization on the characteristics of **4**.

α	M_w (kg.mol^{-1}) [a]	N_{agg} [a]	R_h [b] (nm)	R_c [c] (nm)	Corona Stretching (%) [d]
0	1086	80	10.1	5.6	56
0.1	915	68	9.7	5.3	55
0.25	209	15	5.3	3.2	26
0.5	86	6	4.5	e	e
0.8	16	1	3.2	e	e
1	16	1	2.9	e	e

[a] From SLS at concentrations, M_w is the weight-average molecular weight of the scatterers. [b] Determined from DLS. [c] Calculated from equation 7 assuming a core density of 1. [d] (R_{hDLS}-R_{cSLS})/$L_{contour,DMAEMA}$. [e] For polymers above α = 0.25 the model of "core-corona" is no longer applicable.

Figure S6. Example SLS data plotted as Kc/RΘ versus concentration for **4** at α = 0.
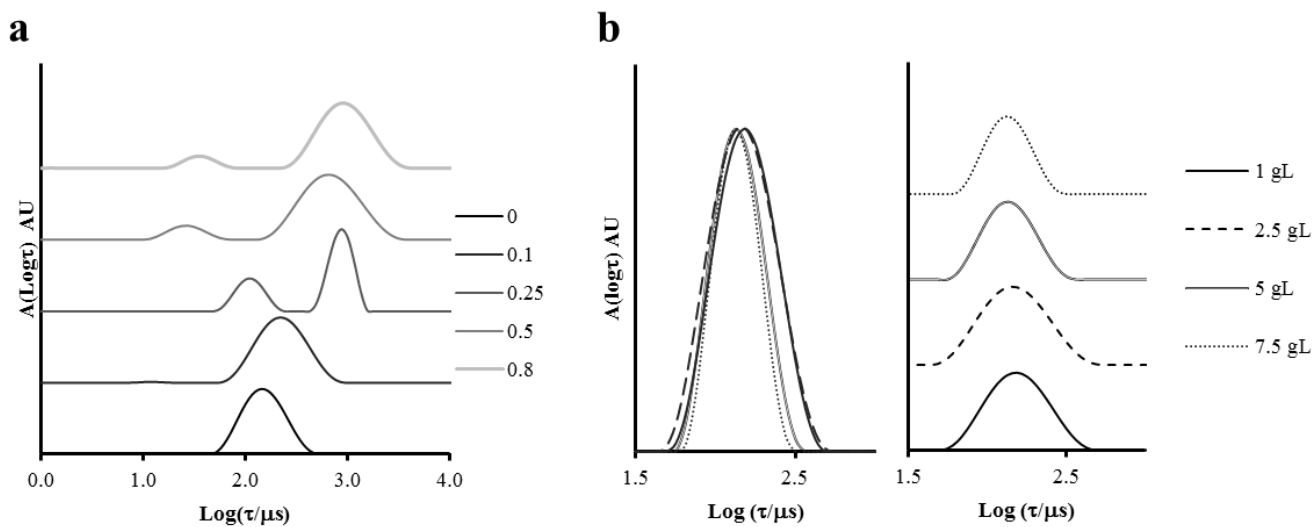

Figure S7. a) Intensity weighted distribution of relaxation times for **3** at 2.5 gL^{-1} in a 0.1 M NaCl solution with varying the ionization, α = 0 – 0.8, measured at θ = 130º. b) Effect of concentration on the intensity weighted distribution of relaxation times for **3**, measured at θ = 130º, α = 0. Note, the distributions have been shifted vertically by a factor of 1.1 to improve clarity.
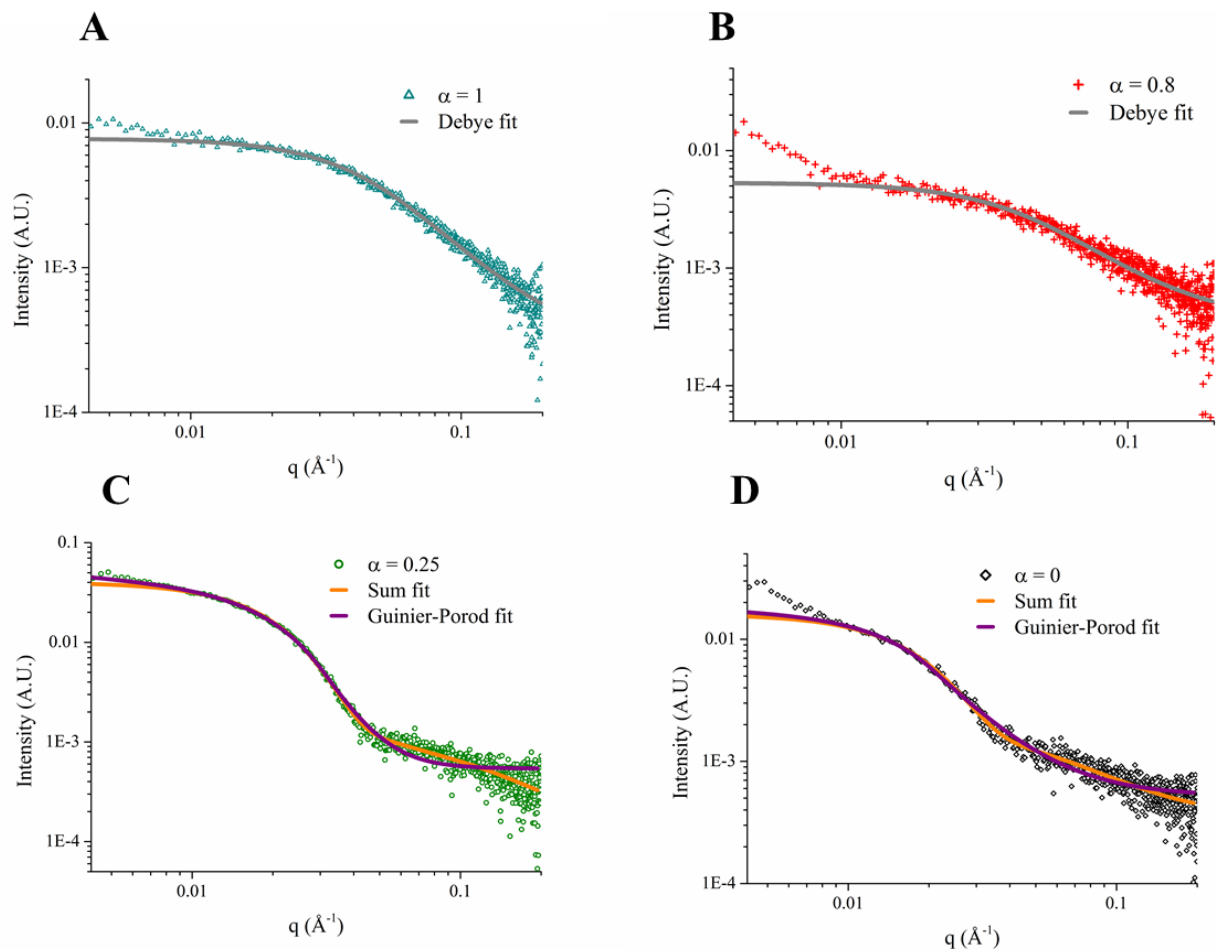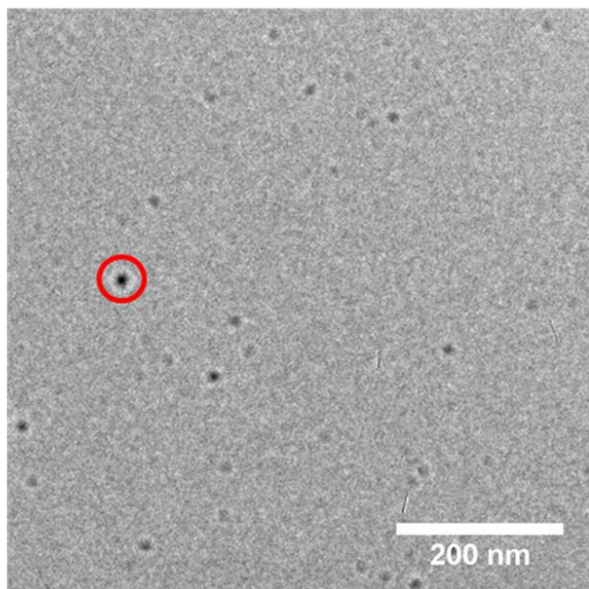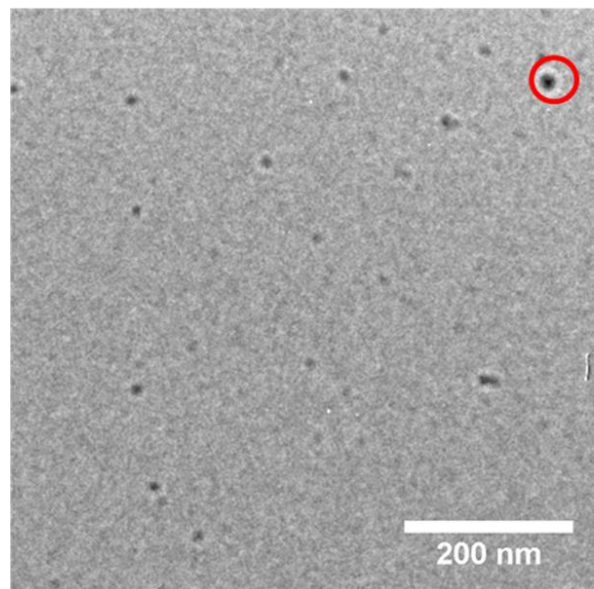
Figure S8. Small-angle X-ray scattering (SAXS) profiles of **3** with varying α. A) α = 1, B) α = 0.8, C) α = 0.25, D) α = 0, all at 2.5 g/L and in 0.1 M NaCl solution.
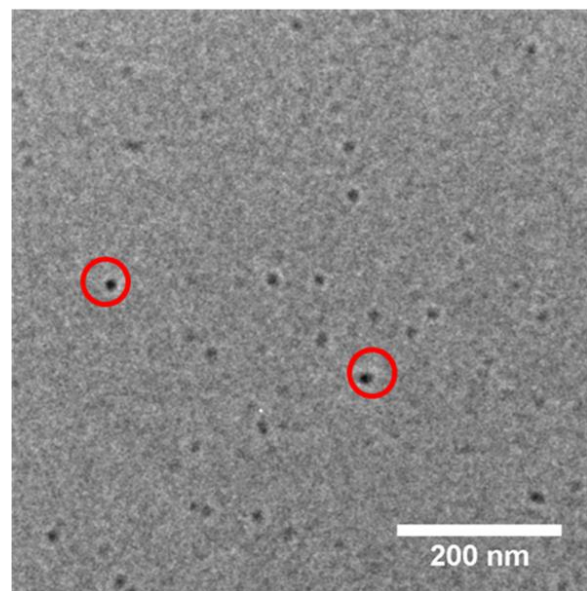
Figure S9. Cryo-TEM images at α = 0, 2g/L and in 0.1 M NaCl solution. a) **2**, b) **3**, c) **4**. Red circles indicate ice crystals. Scale bar 200nm.

Notes and references

[a]University of Warwick, Department of Chemistry, Gibbet Hill Road, Coventry CV4 7AL, UK. Email: R.K.O-Reilly@warwick.ac.uk

[b]LUNAM Université, Université du Maine, IMMM UMR CNRS 6283, Département PCI, Avenue Olivier Messiaen, 72085 Le Mans Cedex 09, France. Email: olivier.colombani@univ-lemans.fr, christophe.chassenieux@univ-lemans.fr

(1)   Van Herk, A. M.; Dröge, T. *Macromol. Theory Simul.* **1997**, *6*, 1263.